ACS APPLIED MATERIALS & INTERFACES

Research Article

www.acsami.org

Nanoscale Piezoelectric Properties of Self-Assembled Fmoc–FF Peptide Fibrous Networks

Kate Ryan,[†,‡] Jason Beirne,[§] Gareth Redmond,[§] Jason I. Kilpatrick,[‡] Jill Guyonnet,[†,‡] Nicolae-Viorel Buchete,[†,∥] Andrei L. Kholkin,[⊥,#] and Brian J. Rodriguez*[,†,‡]

[†]School of Physics, University College Dublin, Belfield, Dublin 4, Ireland

[‡]Conway Institute of Biomolecular and Biomedical Research, University College Dublin, Belfield, Dublin 4, Ireland

[§]School of Chemistry and Chemical Biology, University College Dublin, Belfield, Dublin 4, Ireland

[∥]Complex and Adaptive Systems Laboratory, University College Dublin, Belfield, Dublin 4, Ireland

[⊥]Department of Ceramics and Glass Engineering & CICECO, University of Aveiro, 3810-193 Aveiro, Portugal

[#]Ural Federal University, Lenin Ave. 51, Ekaterinburg 620083, Russia

ABSTRACT: Fibrous peptide networks, such as the structural framework of self-assembled fluorenylmethyloxycarbonyl diphenylalanine (Fmoc–FF) nanofibrils, have mechanical properties that could successfully mimic natural tissues, making them promising materials for tissue engineering scaffolds. These nanomaterials have been determined to exhibit shear piezoelectricity using piezoresponse force microscopy, as previously reported for FF nanotubes. Structural analyses of Fmoc–FF nanofibrils suggest that the observed piezoelectric response may result from the noncentrosymmetric nature of an underlying β-sheet topology. The observed piezoelectricity of Fmoc–FF fibrous networks is advantageous for a range of biomedical applications where electrical or mechanical stimuli are required.

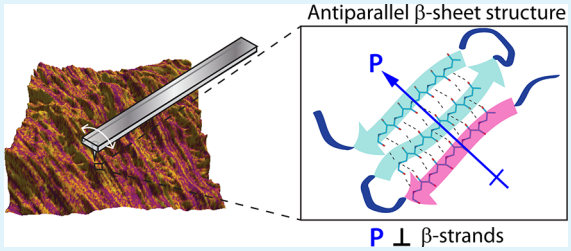

KEYWORDS: *piezoelectricity, peptides, piezoresponse force microscopy, hydrogels, biomaterials*

1. INTRODUCTION

Self-assembling aromatic peptides have an intrinsic ability to form highly ordered nanostructures (i.e., nanospheres, nanotubes, nanofibrils, etc.).[1−4] Spontaneous self-assembly occurs at the nanoscale through conformational packing and linkage between amino acid sequences.[5−7] The presence of aromatic interactions, noncovalent interactions (hydrogen bonds, van der Waals, and electrostatics), and $\pi-\pi$ stacking stabilize the structure with superior stiffness and thermal and chemical stability.[8,9] Additionally, the biological nature of the building blocks facilitates their application to many areas such as biosensing, drug delivery, and tissue engineering.[10]

Diphenylalanine (FF) is a common peptide occurring naturally as the core derivative of amyloid beta (β) protein. It self-assembles into a number of well-characterized nanostructures, including nanotubes, through thermodynamic folding of the β-sheet.[1,2,4,11−13] The β-sheet conformation is the well-established structure of many peptides and proteins, most notably the structure of amyloids, a protein with many functional properties in nature[14] associated with numerous diseases.[15,16] FF nanotubes are widely regarded as useful nanomaterials, exhibiting good thermal, mechanical, and piezoelectric properties.[17,18] Piezoelectricity is an inherent characteristic of noncentrosymmetric materials, whereby electric charge will be generated under mechanical stress or the material will undergo mechanical deformation when subjected to an electric field.[4] The presence of electromechanical coupling in biological systems is an established phenomenon, for example, both neurons and muscle control utilize a voltage-controlled stress or strain mechanism.[19−24] Using piezoresponse force microscopy (PFM), Kholkin et al. have demonstrated that FF nanotubes are piezoelectric, exhibiting shear piezoelectricity along their longitudinal axis attributed to the noncentrosymmetric nature of the β-sheet.[17]

A similar system consists of FF peptides modified with an added fluorenyl-methoxycarbonyl (Fmoc) side group, which self-assembles to form a three-dimensional network of ordered Fmoc–FF nanofibrils via molecular stacking, facilitated by the presence of the Fmoc moiety and mediated by noncovalent interactions.[11,13,25] The Fmoc–FF molecular structure has been suggested to consist of molecules in a β-sheet conformation with a high degree of $\pi-\pi$ stacking.[13,26] The structural similarity of the Fmoc–FF nanofibrils to the piezoelectric FF nanotubes suggests that Fmoc–FF hydrogels may also be piezoelectric.

In general, hydrogels are highly adaptable materials, which can be used to mimic natural tissue, support cell attachment and enhance cell differentiation and survival.[27−29] Fmoc–FF

Received: February 8, 2015
Accepted: May 21, 2015
Published: May 21, 2015

DOI: 10.1021/acsami.5b01251
ACS Appl. Mater. Interfaces 2015, 7, 12702−12707

hydrogels have a structure and viscoelasticity comparable to that of extracellular matrixes and are promising organic materials for tissue engineering applications.[13,25] For example, Liebmann et al. have shown that cells suspended in an Fmoc−FF hydrogel tend to adopt a three-dimensional structure that may more accurately represent cellular shapes in vivo, in contrast to the elongated cellular conformations observed for surface cell cultures.[30] The hydrogels were further shown to have improved biocompatibility for cell cultures as compared to alternative biopolymer materials.[30] Fmoc−FF hydrogels have also been reported to be cytotoxic upon dissolution,[31] highlighting the need to carefully control the parameters of such assays.

In the field of tissue engineering, a scaffold possessing piezoelectric properties could be particularly useful, as bone remodeling and nerve regeneration have both been identified as being sensitive to piezoresponse. The direct piezoelectric effect has been linked with the ability of bone to remodel in response to an applied stress.[22,32,33] Piezoelectricity has also been identified as a precursor to successful axonal regeneration following nerve injury.[34] Therefore, a robust, biocompatible piezoelectric scaffold could provide functional tissue analogues. Here, we investigate piezoelectricity in dried Fmoc−FF peptide hydrogels using PFM.

2. EXPERIMENTAL SECTION

2.1. Peptide Preparation. Fmoc−FF hydrogels were prepared using a solvent-based method.[12,25] Fmoc−FF monomer (B2150, Bachem AG) was dissolved in dimethyl sulfoxide (DMSO) (472301, Sigma-Aldrich) at a concentration of 100 mg mL^{-1}. The hydrogel was subsequently prepared by diluting the stock solution in double distilled H_2O (ddH_2O) to a final concentration of 5 mg mL^{-1} (final hydrogel pH was 4−5).

FF nanotubes were also prepared as a reference sample by dissolving the FF monomer (G-2925 Bachem AG) in lyophilized form in 1,1,1,3,3,3-hexafluoro-2-propanol (105228, Sigma-Aldrich) at a concentration of 100 mg mL^{-1}.[7] The FF stock solution was diluted to a final concentration of 2 mg mL^{-1} in ddH_2O for nanotube self-assembly.

2.2. Photoluminescence (PL) Fmoc−FF Solution and Gel. Fmoc−FF was dissolved in DMSO (1.1 mg mL^{-1}) in a quartz cuvette and using a silicone isolator, 500 μm-thick gel layers were prepared on fused silica (U01-120924-1, University Wafer). PL spectra were acquired using a steady state spectrofluorometer (Quantamaster 40, Photon Technology International, Inc.) using a thin film holder. Acquisition settings of 1 nm step size, 0.1 s integration time, and a 300−900 nm scan range were used. Excitation and emission slits were set to 3 and 1 nm, respectively.

2.3. Circular Dichroism. Circular dichroism (CD) spectra were acquired on a spectropolarimeter (J-810, Jasco Inc.). Five fused silica capillaries (5010S-050, VitroCom) were filled with gel solution, which was allowed to set. Each capillary was sealed with vacuum grease (Dow Corning) and mounted onto a glass frame, which was placed in the path of the light beam. Scans were recorded from 170 to 350 nm, at 5 nm bandwidth and 1 s integration time. The background signal was recorded from blank fused silica capillaries and subtracted to obtain each CD spectrum.

2.4. Attenuated Total Reflectance Fourier Transform Infrared (ATR-FTIR) Spectroscopy. First, 2 mL of gel was deposited onto a zinc selenide horizontal flat plate ATR window (PIKE Technologies, Inc.). The hydrogel layer was allowed to dry onto the window to minimize any water response. The dried sample was then wetted three times with 2 mL of ^2H_2O (D_2O). Scans were performed on a FTIR spectrometer (Cary 680, Agilent Technologies, Inc.) at a resolution of 4 cm^{-1} over 64 accumulations. The background signal was recorded from zinc selenide with D_2O and subtracted to obtain each FTIR spectrum.

2.5. Atomic Force Microscopy and PFM. Contact mode atomic force microscopy (AFM) and PFM measurements (MFP-3D, Asylum Research) were performed using Pt-coated Si cantilevers (MikroMasch CSC37 lever A, HQ:DPE-XSC11 lever B and HQ:DPE-XSC11 lever C with nominal resonant frequencies of 30, 80, and 155 kHz and nominal spring constants of 0.8, 2.7, and 7 N m^{-1}, respectively). A lock-in amplifier (HF2LI, Zurich Instruments) and a high voltage power supply (F10A, FLC Electronics AB) were employed to enable PFM. The cantilevers were calibrated using the thermal noise method and force spectroscopy to establish the spring constant and deflection inverse optical lever sensitivity.[35] The lateral inverse optical lever sensitivity was determined following Peter et al.[36] and taking into account the gain ratio between the deflection and lateral signals (measured to be 4.0 for the AFM used). Uncertainty was estimated as 10% for the deflection inverse optical lever sensitivity, which was then used to calculate errors for all derived values.

Prior to measurements, 20 μL of the samples were deposited on as-received glass slides (631-0907, VWR) and dried under ambient conditions (21 °C, humidity ∼30%) for 24 h, with evaporation aiding the process of self-assembly in the case of the FF nanotubes. An AC voltage was applied to the samples via a conductive tip scanned in contact with the surface with a typical loading force of ∼12 nN and a typical scan rate of ∼0.3 Hz. Lateral PFM (LPFM) was performed using an imaging voltage of 30 V_{rms} applied at a frequency of 5 kHz (to FF sample) and 12.5 kHz (to Fmoc−FF sample). The lock-in amplifier demodulated the cantilever response due to sample deformations into amplitude and phase piezoresponse signals. A 3 ms time constant was used throughout. For measurements of the piezoelectric coefficient,[37] the tip was placed in contact with the surface of both samples with a loading force of 10 nN at specific locations and a 5 kHz (FF sample) and 12.5 kHz (Fmoc−FF sample) AC voltage was swept from 0 to 60 V_{rms} in 6 V_{rms} increments while recording LPFM response.

3. RESULTS AND DISCUSSION

3.1. Structural Characterization. The environment of the Fmoc moiety was monitored by PL to assess the role of intermolecular interactions during peptide aggregation. The solution emission spectrum of Fmoc−FF (i.e., Fmoc−FF/DMSO) had a peak with a maximum intensity at 313 nm (Figure 1). By comparison, the emission spectrum of a gel sample (Fmoc−FF/Hydrogel) showed an intensity maximum at 324 nm.

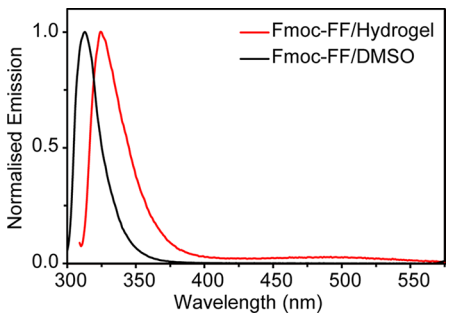

Figure 1. Fluorescence emission spectra measured for Fmoc−FF in solvent and hydrogel phases.

This red-shift of the emission maximum from 313 to 324 nm was likely due to an increase in the dielectric constant of the environment around each fluorenyl chromophore and a transition from free molecules in the solution phase to a more aggregated and organized molecular structure in the gel phase. For example, fluorenyl aggregation could occur via $\pi-\pi$ stacking interactions, possibly with an antiparallel arrangement of the fluorenyl moieties.[13,38] Additionally, the gel PL emission

DOI: 10.1021/acsami.5b01251
ACS Appl. Mater. Interfaces 2015, 7, 12702−12707

spectrum also exhibited a broad feature with a maximum near 500 nm, likely due to emission from fluorenyl excimer species.[39]

To obtain further insight into the nature of the aggregated state in the gel phase, CD spectroscopy was applied to the Fmoc−FF hydrogels (gelation in ddH_2O; Figure 2a). A Cotton

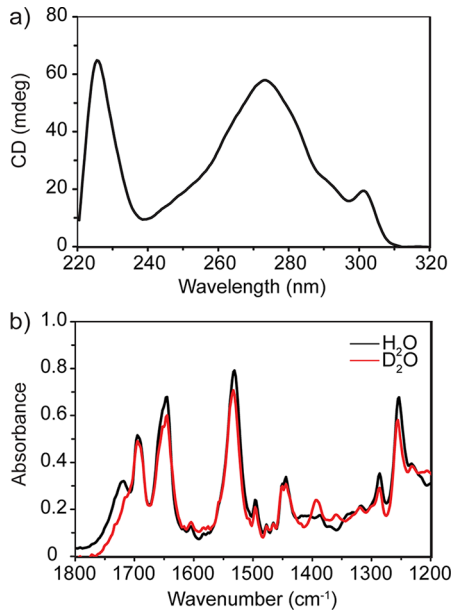

Figure 2. (a) CD spectrum of Fmoc−FF hydrogel and (b) ATR-FTIR spectra of Fmoc−FF hydrogel and Fmoc−FF hydrogel prepared with D_2O.

effect at 226 nm ($n\pi^*$ transition) indicated a superhelical arrangement of the phenylalanine residues, which induced a helical orientation of the fluorenyl moieties (the Cotton effect at 273−301 nm, $\pi\pi^*$ transitions) in the hydrogel.[38,40−42]

More detailed information regarding the arrangement of the Fmoc−FF residues with the hydrogel samples was obtained by acquiring FTIR spectra of hydrogels (gelation in ddH_2O followed by drying and subsequent treatment with D_2O) in attenuated total reflectance mode (Figure 2b). The resulting spectra exhibited distinct spectral bands at 1695, 1645, 1533, and 1255 cm^{-1}. While the feature at 1695 cm^{-1} has in the past been associated with β-turn or antiparallel β-sheet conformations, it has recently also been attributed to carbamate absorption.[43−46] Also, in the amide I region, the peak at 1645 cm^{-1} has previously been reported for materials containing β-sheet, alpha (α)-helical or random coil peptide arrangements, and in the amide II and amide III regions, peaks at 1533 and at 1255 cm^{-1}, respectively, have been associated with either a β-turn or an antiparallel β-sheet secondary structure.[44]

3.2. AFM. The topography of the samples was characterized by contact mode AFM. Topography images of FF nanotubes and dried Fmoc−FF hydrogels are shown in Figure 3a,d. The nanotubes are known to have a wide range of diameters from 100 nm up to several microns.[7,47] The average diameter of the nanotubes in this sample, as determined from their height (Figure 3a), was 667 ± 170 nm (n = 10). The nanofibrils within the dense, layered Fmoc−FF matrix had an average diameter of 66 ± 4 nm (n = 21) (Figure 3d).

3.3. PFM. To characterize the piezoresponse of both samples, we used PFM. This method involves a modified AFM, whereby an electric voltage is applied to the surface via a conducting tip. Using LPFM, piezoelectric deformations can be measured via the torsion of the cantilever. In the case of an FF nanotube lying flat on a substrate, LPFM therefore allows shear deformation to be measured. Previously, Kholkin et al. reported robust LPFM signals, with an expected dependence on the angle between the cantilever and the FF nanotube, for this configuration.[17]

Using LPFM, a piezoelectric response was found in self-assembled FF nanotubes in agreement with literature.[17] The LPFM amplitude and phase images of the FF nanotubes are shown in Figure 3b,c. The LPFM amplitude signal is maximal when the cantilever and nanotube longitudinal axes are orthogonal, such as the nanotube marked by an arrow in Figure 3b. In the LPFM phase image, nanotubes having opposite polarization directions can be identified (the

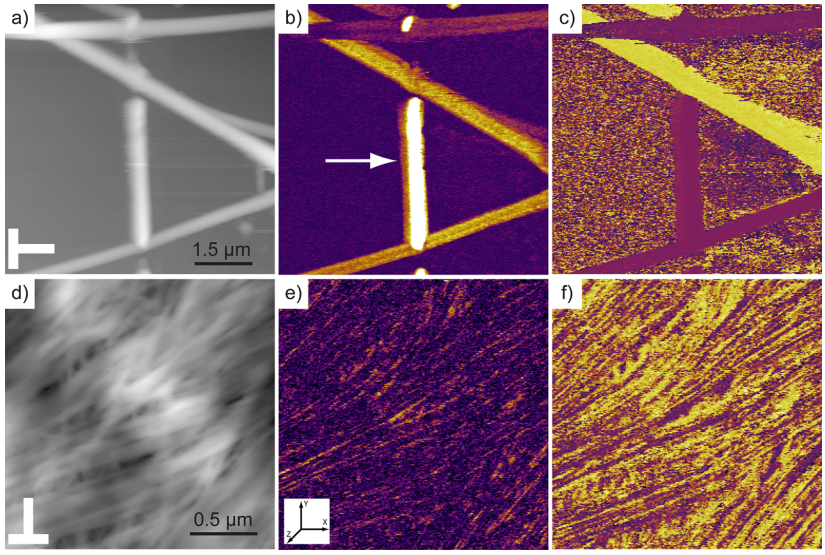

Figure 3. (a and d) AFM topography and LPFM (b and e) amplitude and (c and f) phase images of (a−c) FF nanotubes and (d−e) Fmoc−FF nanofibrils. The Z-scale data ranges are (a) 400 and (d) 80 nm; (b) 200 and (e) 80 pm with both images offset by 150 pm; (c and f) 180°. The arrow in image (b) indicates an FF nanotube orthogonal to cantilever axis. (e, inset) Laboratory coordinate system.

DOI: 10.1021/acsami.5b01251
ACS Appl. Mater. Interfaces 2015, 7, 12702−12707

piezoresponse of purple and yellow nanotubes in Figure 3c have a 180° phase shift).

The LPFM amplitude and phase images for the dried Fmoc–FF hydrogel are shown in Figure 3e,f. The Fmoc–FF nanofibrils within the gel exhibited an apparent shear response, however, strong angle dependency of the LPFM amplitude of the nanofibers was not observed, possibly due to the complex arrangement of the nanofibrils and resolution limits of the technique. In some cases, the phase signal inverts along the length of a fibril, highlighting the heterogeneous nature of the nanofibril network.

As PFM images can contain a background offset signal, in order to quantify the piezoresponse of the FF nanotubes and the Fmoc–FF nanofibrils, the LPFM amplitude was measured as a function of applied voltage (Figure 4). The LPFM signal

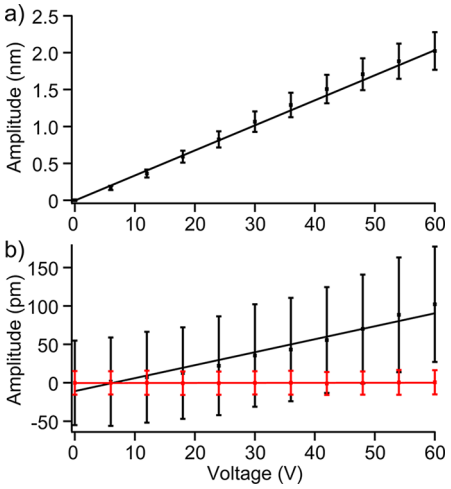

Figure 4. LPFM amplitude versus applied voltage (RMS) recorded on (a) FF nanotubes and (b) Fmoc–FF nanofibrils (black). The slopes provide the average local piezoelectric coefficient, d_{15}^0, for nanotubes and nanofibrils, with an assumed orientation orthogonal to the cantilever. For comparison, the piezoresponse signal measured for a nonpiezoelectric glass slide (red) is shown in (b).

was observed to be linearly dependent on the applied voltage within experimental error. This method provides a value for the d_{35} component of the piezoelectric tensor in the laboratory coordinate system,[48] the measured in-plane effective piezoelectric coefficient obtained from the slope. All measurements carried out on nanotubes and nanofibrils assume that the sample response is orthogonal to the cantilever in the *X*-*Y* plane. Under this assumption, it is possible to directly determine the d_{15} component of the piezoelectric tensor of a shear piezoelectric sample (hereafter called d_{15}^0, where the superscript denotes that the coefficient belongs to the sample coordinate system). The d_{15}^0 for the nanotubes was determined to be 33.7 ± 0.7 pm V^{-1} (n = 5) and for the nanofibrils, d_{15}^0 was determined to be 1.7 ± 0.5 pm V^{-1} (n = 5). The latter is significantly greater than the system detection limits as estimated by measuring d_{35} on nonpiezoelectric glass, which was determined to be 0.002 ± 0.103 pm V^{-1} (n = 5).

3.4. Discussion. The source of piezoelectricity in amyloid fibrils and FF nanotubes is attributed to the collective dipole, or polarization, present due to the arrangement of β-sheets.[23,49,50] Recent atomistic molecular dynamics simulations of FF peptides have shown that individual molecular dipoles depend on the detailed charge state of peptide termini, on the molecular backbone conformational dynamics, as well as on the magnitude of local electric fields.[4] The self-assembly propensity of FF peptides in nanomaterials and their piezoelectric properties are therefore interdependent.[4] Antiparallel β-sheets present dipoles perpendicular to the direction of the β-strands, creating an overall polarization along the fibril/nanotube axis.[51] Mahler et al. have shown that the structure of the Fmoc–FF nanofibrils is consistent with the β-sheet and β-turn conformation present in amyloid fibrils and FF nanotubes.[52] Smith et al. have previously proposed a model structure for the Fmoc–FF nanofibrils, formed from antiparallel β-sheets, whereby the natural twist in the β-sheet leads to the combination of four sheets, creating a cylindrical nanofibril with a typical diameter of ∼3 nm.[13] The available evidence for Fmoc–FF secondary structure indicates that the β-sheet is rolled in a similar fashion with each β-strand perpendicular to the fibril axis, which suggests that a net polarization along the fibril axis could be possible.[51] The nanofibrils observed in this study have an average diameter of 66 ± 4 nm, suggesting the predicted ∼3 nm nanofibrils are in bundles, as has been previously observed for similar materials (e.g., peptide-amphiphiles).[28] These results highlight the ability of potentially biocompatible peptides to form piezoelectrically active structures, which may lead to possible bioapplications.

4. SUMMARY

Fibrous peptide networks composed of self-assembled Fmoc–FF nanofibrils were shown to exhibit shear piezoelectricity by measuring their characteristic local in-plane piezoelectric response using LPFM. Structural characterization suggested that Fmoc–FF nanofibrils present a noncentrosymmetric β-sheet structure, consistent with the mechanism reported for piezoelectric FF nanotubes.[17] Because peptide hydrogels are biomimetic materials with mechanical properties comparable to those of biological gels, the added functionality arising from their piezoelectricity could enable the application of these hydrogels in developing novel piezoelectric scaffolds for tissue engineering.

AUTHOR INFORMATION

Corresponding Author

*E-mail: brian.rodriguez@ucd.ie.

Author Contributions

The manuscript was written through contributions of all authors. All authors have given approval to the final version of the manuscript.

Notes

The authors declare no competing financial interest.

ACKNOWLEDGMENTS

The work is supported by the European Commission within FP7Marie Curie Initial Training Network "Nanomotion" (grant agreement no. 290158). Additional financial support was provided by NANOREMEDIES, which is funded under Cycle 5 of the Programme for Research in Third Level Institutions and cofunded by the European Regional Development Fund. The authors gratefully acknowledge Tim Brosnan for AFM transfer function characterization and Dr. B. Lukasz for assistance with scanning electron microscopy of the cantilevers used. The AFM used for this work was funded by Science Foundation Ireland (SFI07/IN1/B931).

DOI: 10.1021/acsami.5b01251
ACS Appl. Mater. Interfaces 2015, 7, 12702–12707

REFERENCES

(1) Görbitz, C. H. Nanotube Formation by Hydrophobic Dipeptides. *Chem.—Eur. J.* **2001**, *7*, 5153−5159.
(2) Gazit, E. Self-Assembled Peptide Nanostructures: The Design of Molecular Building Blocks and Their Technological Utilization. *Chem. Soc. Rev.* **2007**, *36*, 1263−1269.
(3) Görbitz, C. H. Structures of Dipeptides: The Head-to-Tail Story. *Acta Crystallogr., Sect. B: Struct. Sci.* **2010**, *66*, 84−93.
(4) Kelly, C. M.; Northey, T.; Ryan, K.; Brooks, B. R.; Kholkin, A. L.; Rodriguez, B. J.; Buchete, N.-V. Conformational Dynamics and Aggregation Behavior of Piezoelectric Diphenylalanine Peptides in an External Electric Field. *Biophys. Chem.* **2015**, *196*, 16−24.
(5) Ghadiri, M. R.; Granja, J. R.; Milligan, R. A.; McRee, D. E.; Khazanovich, N. Self-Assembling Organic Nanotubes Based on a Cyclic Peptide Architecture. *Nature* **1993**, *366*, 324−327.
(6) Gazit, E. ChemInform Abstract: The "Correctly Folded" State of Proteins: Is it a Metastable State? *Angew. Chem., Int. Ed.* **2002**, *33*, 257−259.
(7) Reches, M.; Gazit, E. Casting Metal Nanowires Within Discrete Self-Assembled Peptide Nanotubes. *Science* **2003**, *300*, 625−627.
(8) Adler-Abramovich, L.; Kol, N.; Yanai, I.; Barlam, D.; Shneck, R. Z.; Gazit, E.; Rousso, I. Self-Assembled Organic Nanostructures with Metallic-Like Stiffness. *Angew. Chem.* **2010**, *122*, 10135−10138.
(9) Kol, N.; Adler-Abramovich, L.; Barlam, D.; Shneck, R. Z.; Gazit, E.; Rousso, I. Self-Assembled Peptide Nanotubes are Uniquely Rigid Bioinspired Supramolecular Structures. *Nano Lett.* **2005**, *5*, 1343−1346.
(10) Gao, X.; Matsui, H. Peptide-based Nanotubes and Their Applications in Bionanotechnology. *Adv. Mater.* **2005**, *17*, 2037−2050.
(11) Reches, M.; Gazit, E. Self-Assembly of Peptide Nanotubes and Amyloid-Like Structures by Charged-Termini-Capped Diphenylalanine Peptide Analogues. *Isr. J. Chem.* **2005**, *45*, 363−371.
(12) Orbach, R.; Adler-Abramovich, L.; Zigerson, S.; Mironi-Harpaz, I.; Seliktar, D.; Gazit, E. Self-Assembled Fmoc-Peptides as a Platform for the Formation of Nanostructures and Hydrogels. *Biomacromolecules* **2009**, *10*, 2646−2651.
(13) Smith, A. M.; Williams, R. J.; Tang, C.; Coppo, P.; Collins, R. F.; Turner, M. L.; Saiani, A.; Ulijn, R. V. Fmoc-Diphenylalanine Self Assembles to a Hydrogel via a Novel Architecture Based on $\pi-\pi$ Interlocked β-Sheets. *Adv. Mater.* **2008**, *20*, 37−41.
(14) Jarvis, S.; Mostaert, A. *The Functional Fold: Amyloid Structures in Nature*; CRC Press: Boca Raton, FL, 2012.
(15) Gazit, E. Mechanisms of Amyloid Fibril Self-Assembly and Inhibition. *FEBS J.* **2005**, *272*, 5971−5978.
(16) Cherny, I.; Gazit, E. Amyloids: Not Only Pathological Agents but Also Ordered Nanomaterials. *Angew. Chem. Int. Ed.* **2008**, *47*, 4062−4069.
(17) Kholkin, A.; Amdursky, N.; Bdikin, I.; Gazit, E.; Rosenman, G. Strong Piezoelectricity in Bioinspired Peptide Nanotubes. *ACS Nano* **2010**, *4*, 610−614.
(18) Adler-Abramovich, L.; Reches, M.; Sedman, V. L.; Allen, S.; Tendler, S. J. B.; Gazit, E. Thermal and Chemical Stability of Diphenylalanine Peptide Nanotubes: Implications for Nanotechnological Applications. *Langmuir* **2006**, *22*, 1313−1320.
(19) Shamos, M. H. Piezoelectric Effect in Bone. *Nature* **1963**, *197*, 81.
(20) Horiuchi, S.; Tokura, Y. Organic Ferroelectrics. *Nat. Mater.* **2008**, *7*, 357−366.
(21) Zilberstein, R. M. Piezoelectric Activity in Invertebrate Exoskeletons. *Nature* **1972**, *235*, 174−175.
(22) Fukada, E.; Yasuda, I. On the Piezoelectricity of Bone. *J. Phys. Soc. Jpn.* **1957**, *12*, 1158−1162.
(23) Kalinin, S. V.; Rodriguez, B. J.; Jesse, S.; Seal, K.; Proksch, R.; Hohlbauch, S.; Revenko, I.; Thompson, G. L.; Vertegel, A. A. Towards Local Electromechanical Probing of Cellular and Biomolecular Systems in a Liquid Environment. *Nanotechnology* **2007**, *18*, 424020.
(24) Kalinin, S. V.; Rodriguez, B. J.; Jesse, S.; Thundat, T.; Gruverman, A. Electromechanical Imaging of Biological Systems with Sub-10 nm Resolution. *Appl. Phys. Lett.* **2005**, *87*, 3901.
(25) Orbach, R.; Mironi-Harpaz, I.; Adler-Abramovich, L.; Mossou, E.; Mitchell, E. P.; Forsyth, V. T.; Gazit, E.; Seliktar, D. The Rheological and Structural Properties of Fmoc-Peptide-Based Hydrogels: The Effect of Aromatic Molecular Architecture on Self-Assembly and Physical Characteristics. *Langmuir* **2012**, *28*, 2015−2022.
(26) Ulijn, R. V.; Smith, A. M. Designing Peptide Based Nanomaterials. *Chem. Soc. Rev.* **2008**, *37*, 664−675.
(27) McDonald, T.; Patrick, A.; Williams, R.; Cousins, B. G.; Ulijn, R. V. Bio-Responsive Hydrogels for Biomedical Applications. In *Biomedical Applications of Electroactive Polymer Actuators*; John Wiley & Sons, Ltd., Chichester, UK, 2009; pp 43−59.
(28) Smith, L. A.; Ma, P. X. Nano-Fibrous Scaffolds for Tissue Engineering. *Colloids Surf., B* **2004**, *39*, 125−131.
(29) Smith, L. A.; Liu, X.; Ma, P. X. Tissue Engineering with Nano-Fibrous Scaffolds. *Soft Matter* **2008**, *4*, 2144−2149.
(30) Liebmann, T.; Rydholm, S.; Akpe, V.; Brismar, H. Self-Assembling Fmoc Dipeptide Hydrogel for In Situ 3D Cell Culturing. *BMC Biotechnol.* **2007**, *7*, 88.
(31) Truong, W. T.; Su, Y.; Gloria, D.; Braet, F.; Thordarson, P. Dissolution and Degradation of Fmoc-Diphenylalanine Self-Assembled Gels Results in Necrosis at High Concentrations In Vitro. *Biomater. Sci.* **2015**, *3*, 298−307.
(32) Fukada, E. History and Recent Progress in Piezoelectric Polymers. *IEEE Trans. Ultrason., Ferroelect., Freq. Control* **2000**, *47*, 1277−1290.
(33) Denning, D.; Paukshto, M.; Habelitz, S.; Rodriguez, B. J. Piezoelectric Properties of Aligned Collagen Membranes. *J. Biomed. Mater. Res., Part B* **2014**, *102*, 284−292.
(34) Fine, E. G.; Valentini, R. F.; Bellamkonda, R.; Aebischer, P. Improved Nerve Regeneration through Piezoelectric Vinylidenefluoride-Trifluoroethylene Copolymer Guidance Channels. *Biomaterials* **1991**, *12*, 775−780.
(35) Hutter, J. L.; Bechhoefer, J. Calibration of Atomic-Force Microscope Tips. *Rev. Sci. Instrum.* **1993**, *64*, 1868−1873.
(36) Peter, F.; Rudiger, A.; Szot, K.; Waser, R.; Reichenberg, B. Sample-Tip Interaction of Piezoresponse Force Microscopy in Ferroelectric Nanostructures. *IEEE Trans. Ultrason., Ferroelect., Freq. Control* **2006**, *53*, 2253−2260.
(37) Minary-Jolandan, M.; Yu, M.-F. Nanoscale Characterization of Isolated Individual Type I Collagen Fibrils: Polarization and Piezoelectricity. *Nanotechnology* **2009**, *20*, 5706.
(38) Zhang, Y.; Gu, H.; Yang, Z.; Xu, B. Supramolecular Hydrogels Respond to Ligand-Receptor Interaction. *J. Am. Chem. Soc.* **2003**, *125*, 13680−13681.
(39) Schweitzer, D.; Hausser, K. H.; Haenel, M. Transanular Interaction in [2.2]Phanes: [2.2](4, 4′) Diphenylophane and [2.2]-(2,7)Fluorenophane. *Chem. Phys.* **1978**, *29*, 181−185.
(40) Yang, Z.; Gu, H.; Fu, D.; Gao, P.; Lam, J. K.; Xu, B. Enzymatic Formation of Supramolecular Hydrogels. *Adv. Mater.* **2004**, *16*, 1440−1444.
(41) Yang, Z.; Gu, H.; Zhang, Y.; Wang, L.; Xu, B. Small Molecule Hydrogels Based on a Class of Antiinflammatory Agents. *Chem. Commun.* **2004**, 208−209.
(42) Berova, N.; Nakanishi, K.; Woody, R. W.: *Circular Dichroism: Principles and Applications*; Wiley-VCH: New York, 2000; Vol. *912*.
(43) Surewicz, W. K.; Mantsch, H. H.; Chapman, D. Determination of Protein Secondary Structure by Fourier Transform Infrared Spectroscopy: A Critical Assessment. *Biochemistry* **1993**, *32*, 389−394.
(44) Krimm, S. Vibrational Spectroscopy and Conformation of Peptides, Polypeptides, and Proteins. *Adv. Protein Chem.* **1986**, *38*, 181.
(45) Fleming, S.; Frederix, P. W. J. M.; Sasselli, I. R.; Hunt, N. T.; Ulijn, R. V.; Tuttle, T. Assessing the Utility of Infrared Spectroscopy as a Structural Diagnostic Tool for β-Sheets in Self-Assembling Aromatic Peptide Amphiphiles. *Langmuir* **2013**, *29*, 9510−9515.
(46) Eckes, K. M.; Mu, X.; Ruehle, M. A.; Ren, P.; Suggs, L. J. β Sheets Not Required: Combined Experimental and Computational Studies of Self-Assembly and Gelation of the Ester-Containing Analogue of an Fmoc-Dipeptide Hydrogelator. *Langmuir* **2014**, *30*, 5287−5296.

DOI: 10.1021/acsami.5b01251
ACS Appl. Mater. Interfaces 2015, 7, 12702−12707

(47) Rosenman, G.; Beker, P.; Koren, I.; Yevnin, M.; Bank-Srour, B.; Mishina, E.; Semin, S. Bioinspired Peptide Nanotubes: Deposition Technology, Basic Physics and Nanotechnology Applications. *J. Pept. Sci.* **2011**, *17*, 75−87.
(48) Kalinin, S. V.; Rodriguez, B. J.; Jesse, S.; Shin, J.; Baddorf, A. P.; Gupta, P.; Jain, H.; Williams, D. B.; Gruverman, A. Vector Piezoresponse Force Microscopy. *Microsc. Microanal.* **2006**, *12*, 206−220.
(49) Nikiforov, M. P.; Thompson, G. L.; Reukov, V. V.; Jesse, S.; Guo, S.; Rodriguez, B. J.; Seal, K.; Vertegel, A. A.; Kalinin, S. V. Double-Layer Mediated Electromechanical Response of Amyloid Fibrils in Liquid Environment. *ACS Nano* **2010**, *4*, 689−698.
(50) Heredia, A.; Bdikin, I.; Kopyl, S.; Mishina, E.; Semin, S.; Sigov, A.; German, K.; Bystrov, V.; Gracio, J.; Kholkin, A. Temperature-Driven Phase Transformation in Self-Assembled Diphenylalanine Peptide Nanotubes. *J. Phys. D: Appl. Phys.* **2010**, *43*, 462001.
(51) Demirdöven, N.; Cheatum, C. M.; Chung, H. S.; Khalil, M.; Knoester, J.; Tokmakoff, A. Two-Dimensional Infrared Spectroscopy of Antiparallel β-Sheet Secondary Structure. *J. Am. Chem. Soc.* **2004**, *126*, 7981−7990.
(52) Mahler, A.; Reches, M.; Rechter, M.; Cohen, S.; Gazit, E. Rigid, Self-Assembled Hydrogel Composed of a Modified Aromatic Dipeptide. *Adv. Mater.* **2006**, *18*, 1365−1370.

DOI: 10.1021/acsami.5b01251
ACS Appl. Mater. Interfaces 2015, 7, 12702−12707